

Imaging Confined Electrons with Plasmonic Light

Guillaume Schull, Michael Becker, and Richard Berndt

Institut für Experimentelle und Angewandte Physik, Christian-Albrechts-Universität zu Kiel, D-24098 Kiel, Germany

(Received 25 May 2008; published 23 September 2008)

Variations of the spectra of plasmonic light emitted from the junction of a scanning tunneling microscope have been observed for different lateral positions of the scanning tunneling microscope tip on a Au(111) surface. Subnanometer spatial variations of the light emission intensity over a triangular island and in the vicinity of surface step edges have been recorded at different photon energies. They reveal surface standing wave patterns characteristic for two-dimensional confined electrons.

DOI: [10.1103/PhysRevLett.101.136801](https://doi.org/10.1103/PhysRevLett.101.136801)

PACS numbers: 73.20.At, 68.37.Ef, 73.20.Mf, 78.68.+m

Quantum confinement of electrons has been widely studied over the past years. Quantization of electronic states, creation of energy subbands, or extremely high carrier mobilities are fascinating fundamental effects which result from the electron confinement to quantum wells (QWs) [1]. Research on QWs has led to major technological progress, notably in the fabrication of optical devices including laser diodes [2], QW infrared photodetectors [3,4], or QW cascade lasers [5]. Electron gases confined to two dimensions naturally exist at some surfaces where they can be investigated by scanning tunneling microscopy (STM). Lateral oscillations of the surface density of states have been observed due to quantum interferences on the atomic scale, which result from the scattering of the two-dimensional electron gas (2DEG) at inhomogeneities [6–8]. Analogies with optical effects, e.g., quantum mirages, have been reported [9,10], but so far no direct influence of a confined 2DEG on an optical signal has been observed. Here we report the first manifestation of a two-dimensional electron confinement in the plasmonic light emission induced at a STM junction. Subnanometer lateral displacements of the STM tip over an Au(111) surface are used to slightly tune the emission spectra. Energy-resolved maps of the photon emission exhibit standing wave patterns arising from scattering of the 2DEG within quantum resonators or at step edges. These data are direct evidence of inelastic electron tunneling between the STM tip and the 2DEG at the sample surface.

Experiments were performed with an ultrahigh vacuum (UHV) scanning tunneling microscope operating at low temperature (6.8 K). The Au(111) surface as well as chemically etched W tips were cleaned by heating and argon ion bombardment. As a final step to the preparation, the tips were slightly indented to the sample. As a consequence, they are most likely gold coated and exhibit an increased plasmon enhancement compared to pure W tips. Photons emitted at the tunneling junction were recorded by a lens mounted inside the vacuum chamber. The collected light was directed via an optical fiber onto a previously described setup [11] composed of a grating spectrometer

and a liquid nitrogen cooled CCD detector. Spectra are not corrected for detector response.

Light emission from a tunneling junction between metallic electrodes was first reported by Lambe and McCarthy [12]. More recently, the influence of the local density of states of these electrodes on the emitted light has been evidenced [13–15]. This property has been used to probe localized states of atomic wires [16], interband quantum well states transitions [17], and to locally excite fluorescence and phosphorescence of molecules [18–20]. On noble metal surfaces, the light emission occurs through the radiative decay of excited surface plasmons [21,22]. Similar to recent spatially resolved observations of thermally excited plasmons [23], no external illumination is needed to excite the plasmons modes which are, here, excited by the electron current. Model calculations suggest that this phenomenon occurs through the coupling between inelastically tunneling electrons and the electromagnetic field confined within the STM junction [24–26]. Depending on the chemical nature and geometry of both electrodes, the plasmon resonances are excited at different electron energies [25,27,28]. When using the STM tip as an electrode, it becomes possible to resolve the spatial variation of the emission with a resolution equivalent to STM topographies. Figure 1(a) displays two spectra acquired at identical experimental conditions ($V = 1.73$ V, $I = 300$ nA) at two different locations over a triangular island on the Au(111) surface. The peaks observed in these spectra are characteristic of the plasmon resonances of the tip-sample cavity [27–30]. The inset of Fig. 1(a) shows an intriguing difference between these two spectra, and points out a lateral variation of the emitted colors not mentioned in studies realized in similar conditions [14,25,31]. To probe the influence of the tip location on the emitted colors, we recorded spectra simultaneously with topographic imaging. A constant-current STM image acquired at $V = 1.73$ V over a triangular island acting as a quantum resonator is displayed in Fig. 1(b). At each pixel of the image an emission spectrum was recorded [example in Fig. 1(a)]. A spatially resolved "photon map" has been

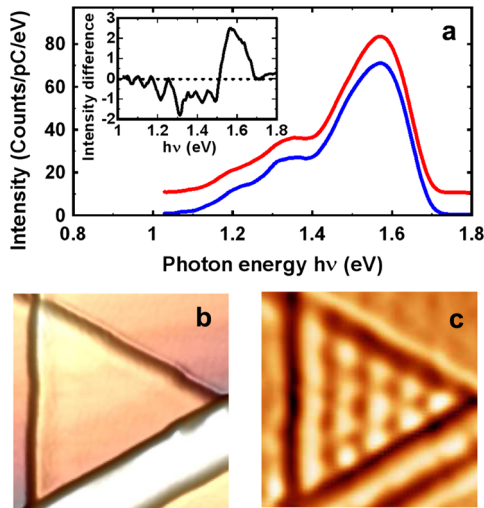


FIG. 1 (color online). (a) Spectra (vertically offset for clarity) of STM-induced light emission from Au(111) obtained at two locations of a triangular island [see image in (b)]. The inset shows the difference between the spectra. (b) $11 \times 11 \text{ nm}^2$ constant-current STM image of a triangular island on Au(111). (c) Energy-resolved ($1.65 < h\nu < 1.7 \text{ eV}$) map of the detected photon intensity (“photon map”) acquired simultaneously with the STM image in (b). Data acquired with a sample bias $V = 1.73 \text{ V}$ and a tunneling current $I = 300 \text{ nA}$.

generated by displaying the intensity from a selected photon energy range [11,32,33] [Fig. 1(c)]. Periodic lateral variations of the light intensity are observed in the photon maps from the triangular resonator. These undulations look similar to density-of-states patterns of confined surfaces state electrons [34].

A similar experiment was performed over a linear step edge of the Au(111) surface for both voltage polarities. Figure 2(a) displays a series of spectra which were recorded along with a topographic scan perpendicular to the step edge. Plotted for each photon wavelength, the dependency of the emitted light intensity is displayed Fig. 2(b) as a function of the distance from the step edge. Here, as in the case of the resonator, standing wave patterns are observed, the wavelength of which varies with photon energy. It is worth noting that the corresponding constant-current STM scans are featureless, owing to the high bias used, which excludes any topographic artifacts in the photon data.

When observed by STM on metal surfaces, standing waves are likely associated to electronic states confined to the surface. For bias voltages in the range $|V| < 1.73 \text{ V}$, the only confined state which may play a role is the Au (111) surface state. We now discuss how this state contributes to the light emission process and analyze the patterns observed in the photon maps. It should be noted that bulk Au states do also contribute to the light emission and give rise to a significant part of the photon emission. However, they cannot explain the undulations discussed here.

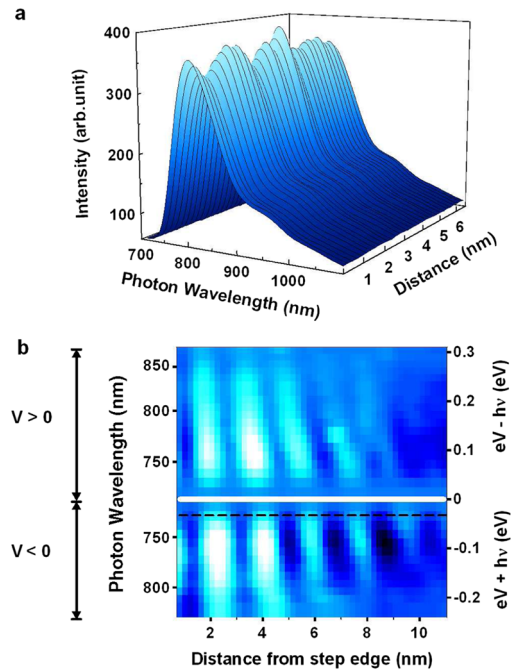


FIG. 2 (color online). (a) Series of light emission spectra recorded during a topographic scan perpendicular to a step edge ($V = -1.73 \text{ V}$). (b) Dependency of the photon intensity plotted for each photon wavelength as a function of the distance from a linear step edge. The top (bottom) panel has been acquired with $V = +1.73$ (-1.73) V. The right abscissa indicates the approximate energy of the surface state electrons involved in the light emission according to the model presented in Fig. 3.

The diagram in Fig. 3(a) represents a tunnel junction at positive sample bias. The surface state dispersion (energy E versus momentum k parallel to the surface) is schematically indicated by a parabola in the junction. The Fermi level of the sample (E_F) is set to 0. We suggest that electrons emit photons when inelastically tunneling from the Fermi level of the tip directly to the surface state of the sample. In this case the surface state affects the density of final states for inelastic tunneling, which implies a relation between the photon energy $h\nu$ and the energy $E(k)$ and, thus, the wave vector k of the final state: $E(k) = eV - h\nu$. In this model, high energy photons result from transitions to the unoccupied surface state close to the Fermi level, i.e., at relatively small k , and photons with smaller $h\nu$ are due to transitions at larger k .

At negative sample bias [Fig. 3(b)] we suggest that electrons tunnel from the occupied part of the surface state, which covers a range of wave vectors and energies, and tunnel inelastically to unoccupied tip states. The energy of the emitted photons depends directly on the energy $E(k)$ of the initial state: $E(k) = eV + h\nu$.

As a preliminary test of this model we extracted a wave vector κ from the photon standing wave patterns by fitting the data in Fig. 2(b) with $1 - J_0(2\kappa x)$ (where J_0 is the

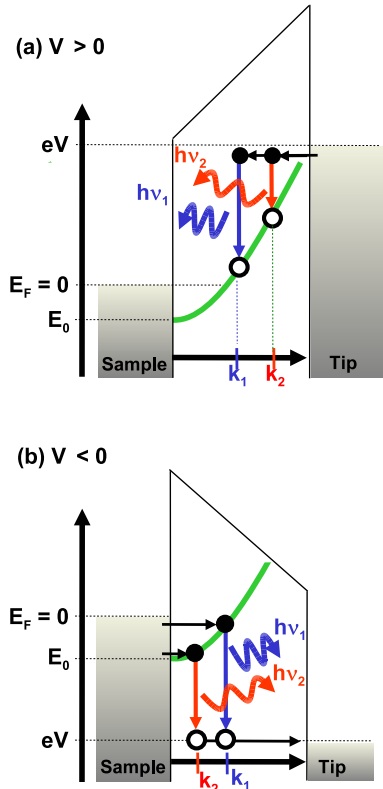


FIG. 3 (color online). Models of the influence of the Au(111) surface state, which is schematically represented by a parabola, on the energy of the emitted photons, for (a) positive and (b) negative sample bias V .

zeroth-order Bessel function and x the distance from the step), similar to the analysis of electronic standing waves [35]. An example is displayed in Fig. 4(a). The influence of a finite lifetime is neglected here since only electronic excitations close to the Fermi level are involved [36]. For $V > 0$ ($V < 0$) Fig. 4(b) displays $eV - h\nu$ versus κ ($eV + h\nu$ versus κ) along with the published dispersion of the Au (111) surface state (dashed line) [37]. Our experimental data (circles) is rather close to the surface state dispersion curve intersecting it around $eV - h\nu = 0$ ($eV + h\nu = 0$), but its slope is higher than expected within this simple analysis.

So far, we have neglected the fact that, at $V > 0$, electrons also tunnel from states below the Fermi level of the tip, increasing the range of initial states. As a result, for a given photon energy $h\nu$, a range of final states and, hence, a range of k , is probed [Fig. 3(a)]. This leads to an increased slope of the experimental dispersion curve. We include this effect in our model by averaging the relevant k , weighted by an energy dependent transmission probability:

$$\bar{k}(h\nu) = \frac{\int_{h\nu}^{eV} T(E)k(E - h\nu)dE}{\int_{h\nu}^{eV} T(E)dE}, \quad \text{for } V > 0. \quad (1)$$

Here $T(E) = \exp[-z\sqrt{\frac{4m}{\hbar^2}(2\Phi + eV - 2E)}]$, $\phi = 4$ eV is

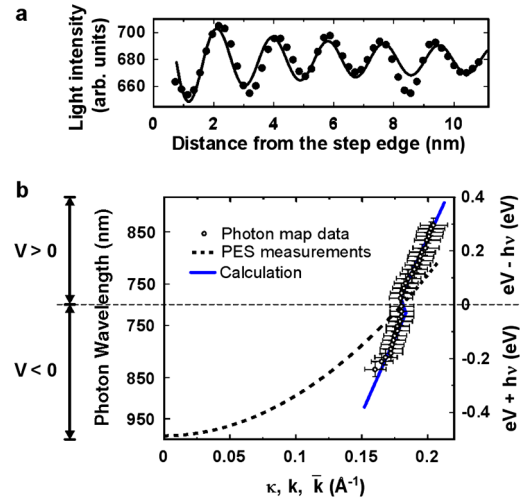


FIG. 4 (color online). (a) Isochromatic light intensity (dots) versus distance from a linear step edge fitted by $1 - J_0(2\kappa x)$ (solid line). [Photon wavelength 725 nm, $V = -1.73$ V, dashed line in Fig. 2(b)]. (b) Dispersion data. Circles: Photon energy $h\nu$ versus wave vector κ extracted from the oscillatory pattern in Fig. 2(b). Horizontal bars reflect the uncertainty of distance measurements in STM images. Vertical bars indicate the photon energy range used. Dashed line: Dispersion (E versus parallel momentum k) of Au(111) surface state as determined by photoelectron spectroscopy (PES) [37]. Solid line: Photon energy $h\nu$ versus averaged wave vector \bar{k} calculated using Eq. (3).

the barrier height for inelastic tunneling which we approximate by the average work function of tip and sample [38]. Similarly, at $V < 0$, for a given $h\nu$, electrons originate from a range of initial states within the occupied part of the surface state. We model this by

$$\bar{k}(h\nu) = \frac{\int_{eV+h\nu}^0 T(E)k(E)dE}{\int_{eV+h\nu}^0 T(E)dE}, \quad \text{for } V < 0. \quad (2)$$

While $\bar{k}(h\nu)$ can easily be calculated numerically, a useful analytical expression may be obtained by a first-order Taylor expansion of \bar{k} in the limit of small $eV \mp h\nu$ for $V > 0$ and $V < 0$, respectively:

$$\bar{k}(h\nu) \approx k_F \left(1 \pm \frac{h\nu \pm eV}{4|E_0|} \right). \quad (3)$$

Here, k_F is the Fermi wave vector of the surface state and E_0 is the energy of the onset of the Au(111) surface state band. Remarkably, this last expression shows that \bar{k} is not influenced by ϕ and z , but to first order depends only on the photon energy and the applied voltage.

Finally, we have to consider the Stark shift of the surface state which is caused by the close proximity of the STM tip and the applied bias and which can be as large as 30 meV at microampere currents [39,40]. We have performed model calculations of the surface state Stark shift as described in Ref. [41]. Considering a tip-sample distance of 1 nm and the voltages used here, we find that E_0 , initially set to -487 mV as measured by photoelectron

spectroscopy [37], is shifted by +25 and −27 mV for positive and negative sample voltage, respectively.

Including these improvements in Eq. (3) we have calculated \bar{k} [Fig. 4(b), solid line] from the known Au(111) surface state dispersion [37] [Fig. 4(b), dashed line]. The good agreement with the dispersion extracted from the emission pattern [Fig. 4(b), circles] confirms the mechanisms proposed in Fig. 3. In agreement with earlier publications which involve rather complex theoretical analyses [24–26], the present measurements constitute unambiguous experimental evidence that plasmonic light emitted at a metallic STM junction is excited by inelastic electron tunneling.

For the first time, a laterally confined two-dimensional electron gas has been probed by inelastic tunneling. Quantum interferences of the 2DEG scattered at step edges were shown to induce modulations of the plasmonic emission. By analogy with QW cascade lasers [5] where the emitted color is tuned by changing the QW thickness, different lateral locations over the quantum interference pattern were used to modify the emission spectra. The possibility to probe the photonic properties of confined electron systems at the atomic scale opens interesting routes towards the realization of single photon sources through the local excitation of unidimensional QW.

We thank Fabrice Charra for fruitful discussions, and Thomas Jürgens for experimental support. We also thank the Deutsche Forschungsgemeinschaft for financial support.

-
- [1] R. Dingle, W. Wiegmann, and C.H. Henry, *Phys. Rev. Lett.* **33**, 827 (1974).
- [2] R. Dingle and C.H. Henry, U.S. Patent No. 3982207, 1976.
- [3] J.S. Smith, L.C. Chiu, S. Margalit, A. Yariv, and A.Y. Cho, *J. Vac. Sci. Technol. B* **1**, 376 (1983).
- [4] B.F. Levine, R.J. Malik, J. Walker, K.K. Choi, C.G. Bethea, D.A. Kleinman, and J.M. Vandenberg, *Appl. Phys. Lett.* **50**, 273 (1987).
- [5] J. Faist, F. Capasso, D.L. Sivco, C. Sitori, A.L. Hutchinson, and A.Y. Cho, *Science* **264**, 553 (1994).
- [6] L.C. Davis, M.P. Everson, R.C. Jaklevic, and W.D. Shen, *Phys. Rev. B* **43**, 3821 (1991).
- [7] M.F. Crommie, C.P. Lutz, and D.M. Eigler, *Nature (London)* **363**, 524 (1993).
- [8] Y. Hasegawa and Ph. Avouris, *Phys. Rev. Lett.* **71**, 1071 (1993).
- [9] H.C. Manoharan, C.P. Lutz, and D.M. Eigler, *Nature (London)* **403**, 512 (2000).
- [10] G. Colas des Francs, Ch. Girard, J.-C. Weeber, C. Chicane, Th. David, A. Dereux, and D. Peyrade, *Phys. Rev. Lett.* **86**, 4950 (2001).
- [11] G. Hoffmann, J. Kröger, and R. Berndt, *Rev. Sci. Instrum.* **73**, 305 (2002).
- [12] J. Lambe and S.L. McCarthy, *Phys. Rev. Lett.* **37**, 923 (1976).
- [13] R. Berndt and J.K. Gimzewski, *Phys. Rev. B* **48**, 4746 (1993).
- [14] K. Perronet, L. Barbier, and F. Charra, *Phys. Rev. B* **70**, 201405(R) (2004).
- [15] G. Hoffmann, T. Maroutian, and R. Berndt, *Phys. Rev. Lett.* **93**, 076102 (2004).
- [16] G.V. Nazin, X.H. Qiu, and W. Ho, *Phys. Rev. Lett.* **90**, 216110 (2003).
- [17] G. Hoffmann, J. Kliever, and R. Berndt, *Phys. Rev. Lett.* **87**, 176803 (2001).
- [18] X.H. Qiu, G.V. Nazin, and W. Ho, *Science* **299**, 542 (2003).
- [19] Z.-C. Dong, X.-L. Guo, A.S. Trifonov, P.S. Dorozhkin, K. Miki, K. Kimura, S. Yokoyama, and S. Mashiko, *Phys. Rev. Lett.* **92**, 086801 (2004).
- [20] E. Cavar, M.-C. Blüm, M. Pivetta, F. Patthey, M. Chergui, and W.-D. Schneider, *Phys. Rev. Lett.* **95**, 196102 (2005).
- [21] J.K. Gimzewski, J.K. Sass, R.R. Schlittler, and J. Schott, *Europhys. Lett.* **8**, 435 (1989).
- [22] Y. Uehara, Y. Kimura, S. Ushioda, and K. Takeuchi, *Jpn. J. Appl. Phys.* **31**, 2465 (1992).
- [23] Y. De Wilde, F. Formanek, R. Carminati, B. Gralak, P.-A. Lemoine, K. Joulain, J.P. Mulet, Y. Chen, and J.-J. Greffet, *Nature (London)* **444**, 740 (2006).
- [24] P. Johansson, R. Monreal, and P. Apell, *Phys. Rev. B* **42**, 9210 (1990).
- [25] R. Berndt, J.K. Gimzewski, and P. Johansson, *Phys. Rev. Lett.* **67**, 3796 (1991).
- [26] B.N.J. Persson and A. Baratoff, *Phys. Rev. Lett.* **68**, 3224 (1992).
- [27] J. Aizpurua, S.P. Apell, and R. Berndt, *Phys. Rev. B* **62**, 2065 (2000).
- [28] K. Meguro, K. Sakamoto, R. Arafune, M. Satoh, and S. Ushioda, *Phys. Rev. B* **65**, 165405 (2002).
- [29] C. Maurel, R. Coratger, F. Ajuston, G. Seine, R. Péchou, and J. Beauvillain, *Surf. Sci.* **529**, 359 (2003).
- [30] N. Nilius, N. Ernst, and H.-J. Freund, *Phys. Rev. B* **65**, 115421 (2002).
- [31] Y. Uehara, T. Fujita, and S. Ushioda, *Phys. Rev. Lett.* **83**, 2445 (1999).
- [32] R. Nishitani, T. Umeno, A. Kasuya, and Y. Nishina, *Surf. Rev. Lett.* **4**, 1009 (1997).
- [33] A. Downes, P. Guaino, and P. Dumas, *Appl. Phys. Lett.* **80**, 380 (2002).
- [34] K.-F. Braun and K.-H. Rieder, *Phys. Rev. Lett.* **88**, 096801 (2002).
- [35] Ph. Avouris, I.-W. Lyo, R.E. Walkup, and Y. Hasagawa, *J. Vac. Sci. Technol. B* **12**, 1447 (1994).
- [36] L. Bürgi, O. Jeandupeux, H. Brune, and K. Kern, *Phys. Rev. Lett.* **82**, 4516 (1999).
- [37] F. Reinert, G. Nicolay, S. Schmidt, D. Ehm, and S. Hüfner, *Phys. Rev. B* **63**, 115415 (2001).
- [38] J. Aizpurua, G. Hoffmann, S.P. Apell, and R. Berndt, *Phys. Rev. Lett.* **89**, 156803 (2002).
- [39] L. Limot, T. Maroutian, P. Johansson, and R. Berndt, *Phys. Rev. Lett.* **91**, 196801 (2003).
- [40] J. Kröger, L. Limot, H. Jensen, R. Berndt, and P. Johansson, *Phys. Rev. B* **70**, 033401 (2004).
- [41] M. Becker, S. Crampin, and R. Berndt, *Phys. Rev. B* **73**, 081402(R) (2006).